

NASA Technical Memorandum 107309
AIAA-96-2622

Metallized Gelled Propellants: Oxygen/RP-1/ Aluminum Rocket Heat Transfer and Combustion Measurements

Bryan Palaszewski
*Lewis Research Center
Cleveland, Ohio*

and

James S. Zakany
*NYMA, Inc.
Brook Park, Ohio*

Prepared for the
32nd Joint Propulsion Conference
cosponsored by AIAA, ASME, SAE, and ASEE
Lake Buena Vista, Florida, July 1-3, 1996



National Aeronautics and
Space Administration

METALLIZED GELLED PROPELLANTS: OXYGEN /RP-1 /ALUMINUM ROCKET HEAT TRANSFER AND COMBUSTION MEASUREMENTS

Bryan Palaszewski*
NASA Lewis Research Center
Cleveland, OH 44135

James S. Zakany
NYMA, Inc.
Lewis Research Center Group
Brook Park, OH 44142

Abstract

A series of rocket engine heat transfer experiments using metallized gelled liquid propellants was conducted. These experiments used a small 20- to 40-lb_f thrust engine composed of a modular injector, igniter, chamber and nozzle. The fuels used were traditional liquid RP-1 and gelled RP-1 with 0-, 5-, and 55-wt% loadings of aluminum particles. Gaseous oxygen was used as the oxidizer. Three different injectors were used during the testing: one for the baseline O₂/RP-1 tests and two for the gelled and metallized gelled fuel firings. Heat transfer measurements were made with a rocket engine calorimeter chamber and nozzle with a total of 31 cooling channels. Each channel used a water flow to carry heat away from the chamber and the attached thermocouples and flow meters allowed heat flux estimates at each of the 31 stations. The rocket engine Cstar efficiency for the RP-1 fuel was in the 65-69% range, while the gelled 0-wt% RP-1 and the 5-wt% RP-1 exhibited a Cstar efficiency range of 60 to 62% and 65 to 67%, respectively. The 55-wt% RP-1 fuel delivered a 42-47% Cstar efficiency. Comparisons of the heat flux and temperature profiles of the RP-1 and the

metallized gelled RP-1/Al fuels show that the peak nozzle heat fluxes with the metallized gelled O₂/RP-1/Al propellants are substantially higher than the baseline O₂/RP-1: up to double the flux for the 55-wt% RP-1/Al over the RP-1 fuel. Analyses showed that the heat transfer to the wall was significantly different for the RP-1/Al at 55-wt% versus the RP-1 fuel. Also, a gellant and an aluminum combustion delay was inferred in the 0% and 5-wt% RP-1/Al cases from the decrease in heat flux in the first part of the chamber. A large decrease in heat flux in the last half of the chamber was caused by fuel deposition in the chamber and nozzle. The engine combustion occurred well downstream of the injector face based on the heat flux estimates from the temperature measurements.

Nomenclature

Al	Aluminum
Cstar	Characteristic velocity (m/s)
°F	Fahrenheit degrees
I _{sp}	Specific Impulse (lb _f -s/lb _m)
IRFNA	Inhibited Red Fuming Nitric Acid
K	Kelvin
MMH	Monomethyl Hydrazine
O ₂	Oxygen

* AIAA Senior Member, Program Manager,
Fuels and Space Propellants for Reusable
Launch Vehicles - Small Business Innovation
Research (SBIR) Focused Topic

lbf	pound-force
Q/A	Heat flux (MW/m ²)
RP-1	Rocket Propellant-1
T	Temperature (K or °F)
wt%	Weight Percent of Fuel Mass

scale engine, but the data would nonetheless help guide future large-scale testing efforts. These experiments were also done to identify conditions or metal loadings that will provide better efficiency and other information that will improve the thinking in future trade studies.

Introduction

Experimental rocket engine heat transfer and combustion measurements were conducted with metallized gelled O₂/RP-1/Al. Three different gelled fuels were used including 0-, 5-, and 55-wt% RP-1/Al. Traditional RP-1 was used as the basis of comparison. A water-cooled calorimeter chamber and nozzle were used to measure the heat flows in the rocket engine. Traditional 4- and 8-element triplet injectors with oxidizer on the outer flow paths (O-F-O) were used. Three injectors were used: two were designed for metallized gelled propellants and one for the traditional RP-1. The calorimeter engine hardware and injector designs were derived from NASA Lewis' past programs. These tests were planned to determine the potential metal combustion lag caused by aluminum combustion in the multi-phase flow typical of metallized gelled propellants. They were also planned as a follow-on to the previously conducted heat sink rocket engine testing to provide data that would improve future test engine designs and test programs with metal and gellant combustion in rocket propellants.

After the initial heat sink engine tests, added testing was conducted with a calorimeter chamber and nozzle to find any effects of propellant combustion delay due to the multi-phase fluid in the chamber with the metal particles. As with the heat sink tests, the other purpose of the experiments was to determine the realistic combustion efficiency one might expect for O₂/RP-1/Al metallized gelled fuels and to see if a rocket combustor could deliver the relatively high efficiency needed for successful NASA applications of metallized gelled combustion. Facility limits restricted the testing to a small combustor, so the efficiency might not be as high as predicted for a full-

Background

Metallized gelled liquid fuels have the potential for increasing the specific impulse, the density, and the safety of rocket propulsion systems.¹⁻¹⁶ While the benefits and military applications of Earth-storable (IRFNA/MMH) gelled and metallized gelled fuels and oxidizers are well established, some questions still exist regarding their application for NASA missions. Oxygen /RP-1 /Al and cryogenic metallized gelled propellants show promise in the design studies for NASA missions, assuming an engine efficiency comparable to traditional liquid fuels. In the mission studies, there was a relatively limited range of efficiency where metallized propellants were most effective in reducing booster size and improving delivered payload. Experimental efforts to resolve the performance issue were therefore planned and conducted. The questions that arose prior to and during these investigations include: can propellants be fired successfully in a rocket engine, what is the combustion efficiency, are the metallized gelled propellants easily controlled, and are their flow properties predictable? The NASA experimental work^{15, 16} was applicable to small 20- to 40-lbf rocket engines and was a first step toward answering these questions. While all of the mentioned issues have not been fully addressed for all thrust levels, the data from these tests can guide future research and help pave the way for successful future testing.

This work was conducted in conjunction with the heat sink engine testing discussed in References 15 and 16. The heat sink testing showed that a rocket engine can be fired successfully, that the propellant flow is controllable and that the flow properties are predictable. Rocket engine performance was

an issue, due to the small size of the engine and the relatively large purge flow rates needed to make the engine firing repeatable. Questions also arose in terms of the propellant exposure to air and drying in the feed system and injector. Many issues were resolved in the heat sink testing, but solutions to the igniter purge effects were not able to be implemented in the past test program.

Why Metallized Gelled Propellants?

Metallized gelled propellants have been studied analytically and experimentally for over 60 years¹. The historical work has focused on the benefits of high specific impulse, high density, and safety^{2, 3, 4, 5, 6}. Current non-NASA uses for these propellants may lie in tactical and strategic missiles and aircraft ejection seats^{3, 4, 5, 6}. Extensive work has been conducted with metallized-gelled Earth-storable propellants, such as hydrazine (N_2H_4), Inhibited Red Fuming Nitric Acid (IRFNA), and monomethyl hydrazine (MMH).^{4, 5, 6} However, these propellants are not planned for use in future NASA launch vehicles. To explore the potential of metallized-gelled fuels, NASA chose to pursue the propellant combinations that were more suitable to its future plans in the Metallized Propellant Program⁷⁻¹⁶. This program, at the NASA Lewis Research Center, has been conducting experimental, analytical, and mission studies since 1987. This program has concentrated on $O_2/RP-1$ and O_2/H_2 propellant combinations and the issues related to using these gelled propellants with metal particle additives.

A series of propulsion and vehicle trades studies^{7, 11, 12, 13, 14} had shown a potential benefit for metallized gelled fuels for NASA launch vehicles and have indicated that $O_2/RP-1/Al$ can have significant benefits by increasing propellant density. Figure 1, which is derived from data in Reference 11, depicts the potential increases in payload enabled by high-density 55-wt% $RP-1/Al$. Using $O_2/RP-1/Al$ propellants in a Liquid Rocket Booster replacement of the Space Shuttle Solid Rocket

Boosters (SRB)^{7, 11, 15}, the propellant density increase allows for shorter boosters. Alternatively, for the same booster size, $O_2/RP-1/Al$ has the potential for higher payload delivery mass over traditional solid propellants. With $O_2/RP-1/Al$, the specific impulse is lower than that for $O_2/RP-1$ propellants, even for the highest payload benefit cases. This payload benefit is enabled because the high density of the gelled metallized fuel allows a larger mass of propellant to be placed in a smaller volume than traditional liquid propellants. Gelled propellants' thixotropic nature also increases safety by minimizing the potential for tank leakage and reduces the spill area in case of an accidental propellant release.

Based on rocket engine and vehicle performance studies, 0-, 5-, and 55-wt% aluminum loadings in $RP-1$ seemed the most attractive¹¹. During the course of these investigations, it became clear that gelled fuels may be more attractive to users than those with metal particles. A stepping-stone approach where gelled fuels are first used and then the users evolve toward metallized gelled propellants is a definite option. Future vehicles using gelled fuels may allow for slosh reduction, added safety, and leakage reduction. Therefore, gelled $RP-1$ (0 wt%) was one of the selected candidates. The 0-wt% loading provided a basis of comparison to estimate the gains or losses of gelling the $RP-1$. Based on a parametric engine performance analysis, the 5-wt% loading delivered the maximum predicted I_{sp} for the $O_2/RP-1/Al$ combinations. This was one reason for the selection of this metal loading. Another reason is that, based on design of experiments methodologies, the selection of three different metal loadings would show the relative trends in performance, and allow the data to be compared to the theoretical trends.

Experiment Objectives

Rocket performance and heat transfer measurements were desired in this test program. Since no data were previously available for $O_2/RP-1/Al$ rocket combustion

heat transfer, rocket calorimeter measurements were sought and obtained. Testing was therefore conducted with O₂/RP-1/Al propellants using gelled RP-1 with aluminum particles. During the combustion of metal particles, the multi-phase flow creates a distribution of liquid, solid and gas in the combustion chamber. There is therefore a mismatch in the combustion time scale of the gas, the liquid or gelled droplets and the solid particles. The heat transfer measurements were envisioned so that some estimate might be made of the metal combustion lag for the aluminum. Both baseline non-metallized propellants and various metal loadings with gelled RP-1 were used to compare the combustion temperature heat flux profiles of the different combustion environments. The results of the related heat sink engine testing are summarized in References 15 and 16 and the rocket heat transfer profiles as well as their associated combustion performance in the rocket engine are presented in this paper.

Experimental Setup: Fuels and Rocket Engine

Fuel Preparation

Several types of metallized gelled fuels with different metal loadings were investigated. Based on rocket engine and vehicle performance studies, 0-, 5-, and 55-wt% aluminum loadings in RP-1 seemed the most attractive. The 0-wt% loading provided a basis of comparison to estimate the gains or losses of gelling the RP-1 and the 5-wt% loading delivered the maximum theoretical I_{sp} for the O₂/RP-1/Al combinations.

All of the propellant mixing was conducted in Cell 14 of the NASA Lewis Rocket Laboratories. Table I provides the constituents of the different fuels. The gelled RP-1 was prepared with a 6.5-wt% gellant concentration. This gellant wt% was selected based on a series of gelling experiments in which a range of 1-10 wt% gellant was used. With the 5 wt% RP-1/Al fuel, 5 wt% gellant was added and with the 55 wt% RP-1/Al, the

gellant fraction was 3.5 wt%. When mixing, it is important to add the "dry" elements first: adding metal, then gellant, then fuel. A very small wt% of liquid surfactant, Tween 85, was also added as the last component to the 55-wt% metal loaded fuel. The surfactant aids the formation of the gel network when using a high metal loading. The dry components are also very powdery, requiring respirator use.

The gelled metallized propellant density is computed using:

Gel Density (kg/m³) =

$$\frac{1}{\frac{(1 - ML)}{\text{RP-1 Density}} + \frac{ML}{\text{Al Density}} + \frac{\text{SiO}_2 \text{ Loading}}{\text{SiO}_2 \text{ Density}}}$$

where:

ML weight fraction of metal (Al) in the total weight of fuel

SiO₂ Loading weight fraction of gellant (SiO₂) in the total weight of fuel

The surfactant is only 0.7% of the mass of the metallized gelled fuel, so it was not included in the above equation.

One-half gallon batches of the fuel were prepared in storage cans. A paint rejuvenator (or shaker) was used to mix the fuel components. The fuel mixing can was typically half filled to allow for more effective mixing of the components during the shaking process.

To place the gelled fuel into the piston-cylinder tank, a transfer tank system was constructed and consisted of a 10 gallon pressure vessel that was rated for 150 psig. The gelled fuel was poured into the transfer tank, and after sealing the tank, it was pressurized to about 70 psig with nitrogen. Nitrogen was used because gelled fuels will dry when exposed to air. Much effort was

exercised to minimize the fuel's air exposure prior to actual rocket testing.

Combustion Testing Description

All of the combustion experiments were conducted in Cell 21 of NASA Lewis Rocket Laboratories which is configured to test low thrust rocket engines (nominally 50 pounds of thrust) at sea level or altitude conditions. Only minor modifications to the cell were necessary to safely handle the gelled RP-1/Al propellant mixtures and to capture the exhaust products for analysis and disposal. A propellant feed subsystem was installed in Cell 21 to supply the engine with gelled metallized propellant. The main component of this system was a high pressure hydraulic piston-cylinder. This piston-cylinder was fed with the propellant mixture from a pressurized transfer tank. A schematic of the charging system is shown in Figure 2. The piston cylinder was pressurized with hydraulic fluid. Propellant flow was regulated by limiting the flow of hydraulic fluid into the piston-cylinder. This was accomplished by controlling the fluid pressure upstream of a cavitating venturi. The results of this method were that the propellant remained fluid and its mass flow rate was held very constant. Variations in the fuel mass flow rate under different engine conditions were manageable. Throughout most of the test matrix, the fuel feed system parameters were kept constant and the oxidizer load pressures were changed to achieve various propellant mixture ratios. Another modification to the test cell was the addition of an exhaust recovery system. This modular system of scrubbers, pumps, and collection filters allowed the experiment to be accomplished with far less environmental impact than any similar test before it in this facility. Since the exhaust products were collected, they could easily be examined for further data concerning the combustion of the fuel mixtures.

Except for the RP-1 and RP-1/Al, all of the propellants in the cell are provided in gaseous form. The gases are O₂, H₂, and N₂. Both the O₂ and H₂ are used for the engine igniter and are provided from high-pressure

trailers. Nitrogen is used as a purge gas to protect the igniter and engine after engine shutdown. The liquid RP-1 propellant is delivered to the engine using an 8-gallon pressurized tank attached to the cell. Gelled propellants are pressurized and fed using a piston-cylinder tank. Mass flow rates of the propellants were measured by Coriolis-type mass flow meters, in the case of RP-1 and the gelled propellants, and by pressure transducer outputs coupled with choked jeweled orifices in the feed lines in the case of gaseous propellants. Flow of the liquid RP-1 propellant was limited by cavitating venturis. In all cases, upstream load pressures have a direct bearing on the mass flow rates of the propellant. The test matrix conditions were satisfied by varying these load pressures and by changing the flow control devices.

Several data acquisition systems were employed to provide the cell operator and the researcher with timely and complete data. High fidelity research data was collected with a high speed (TRADAR 2.5) computer system. The high speed data acquisition system is used for highly transient rocket engine measurements of chamber pressure and engine propellant manifold pressures and TRADAR provides a 50 kHz sampling rate with 100 data channels. Immediate performance data was available on the strip-chart data logging chart recorder. This recorder could display up to 16 channels of data sampled at 200 kHz. Steady state data was collected and presented by the low speed (ESCORT) system, with a 1 second sampling rate. The low speed system was used to record more steady state data on propellant line and tank pressures and temperatures. This system supports over 100 channels. In addition to digital data, each run was recorded by a video camera and saved on video tape. Selected runs were also filmed with a high speed film camera at 2000 frames per second. Several still photographs were taken between and during each run. Extensive photographic records were collected of the test hardware before and after run sets.

Engine Hardware

Rocket engine calorimeter chamber and nozzle experiments were conducted. The calorimeter combustion chamber had a 2.6-inch inside diameter, was 5.875 inches long, and the calorimeter nozzle had a 0.6-inch diameter throat. The maximum expansion ratio of the nozzle was 4.77:1, though for consistency with the heat sink calculations and measurements, the expansion ratio used in the analysis was 2.4:1. Figure 3 shows a simple diagram of the engine configuration. In conducting these tests, hardware was desired to be modular so that many injector options could be tested. Also, any damaged hardware could be removed and easily replaced.

A total of 22 cooling channels were built into the calorimeter chamber and the calorimeter nozzle had 9 cooling circuits. Table II provides the locations of each station in the chamber and nozzle. Numerous thermocouples are located in the cooling passages of the calorimeter combustion chamber. Two thermocouples were used per cooling circuit. Multiple thermocouples were desired to find any changes in the chamber temperature perimeter. Temperature measurements were also made for the water entering and exiting the cooling channels. These measurements were the primary method of estimating the heat flux in each channel. Standard heat transfer calculations are performed with this data to estimate the heat flux at each station.¹⁷⁻²⁰ During operation, the engine uses a water flow of 0.1-1.0 gallons per minute in each of 31 flow channels. The flow meters were of a turbine type and a venturi type (using a pressure difference (ΔP) transducer) and were used to measure the water flow rates. The turbine flow meters measured the water flow rates in the cooling channels and with the thermocouple data on the inlet and outlet temperature of each channel, the heat flux was calculated. The heat transfer results from the channels with the turbine flow meters were compared to the heat fluxes computed with the adjacent venturi flow meters' measurements (with the ΔP transducers). The number of the

water feed lines, thermocouples, and flow meters needed in the 31 channels for the heat transfer measurements is high and great care is needed to assure the data reflect the proper heat transfer locations. Approximately one month was required for one technician to setup the calorimeter engine and its measurement devices.

The injectors use an oxidizer manifold within the injector body and have a fuel dome set atop it. The injector elements used an O-F-O triplet design and both four- and eight-element patterns were tested. The elements were arranged to be mutually perpendicular. Due to the use of a gelled metallized fuel, there is the potential of the RP-1 evaporating and the remaining mix of particles and gellant drying in the fuel passages. Using a removable fuel dome minimized the potential of propellant particles being trapped in a complex set of flow passages in the internal body manifold. During the testing, a wide range of oxidizer-fuel ratios (O/F) were investigated. The injectors were designed for an O/F range of 1.2-4.2 for O_2 /RP-1 and 1.4-3.7 for O_2 /RP-1/Al.

The igniter assembly consisted of a 3.437 cm^3 (0.210 in^3) volume hydrogen-oxygen mixing chamber, a spark igniter, and a 0.475 cm (0.187 in) diameter flame propagation tube. Hydrogen and oxygen entered the mixing chamber through opposing inlets. Hydrogen was also directed along the exterior of the flame propagation tube to cool it. A high O/F ratio was maintained in the igniter assembly to reduce the flame temperature. The excess hydrogen ported along the exterior of the flame propagation tube reduced the local O/F ratio near the injector face, resulting in a much hotter ignition flame.

Engine Mounting, Start Up, and Shutdown

The engine, including the injector, igniter, chamber and nozzle, was mounted to the test stand with stainless steel rods that are screwed into and protrude from the injector body. All of the engine components were

assembled with threaded bolts. Three metal seals and one elastomeric O-ring are needed for assembling and sealing the engine components. After the engine is mounted in the test stand, the major connections are for the primary fuel and oxidizer manifolds, the igniter fuel and oxidizer and the purge flows for all of the flow paths except the primary fuel. A typical ignition sequence begins with the O_2/H_2 torch igniter firing for 1 second, and after 0.2 to 0.4 seconds of operation, the fuel and oxidizer are turned on, with a 0.2 to 0.3 second fuel lead.

After main engine ignition has occurred, the igniter flow is shut off and a nitrogen purge is initiated to prevent the igniter from being consumed by the main combustion flow. This purge flow pressure is a minimum of 30 psi higher than the main chamber pressure to assure that no combustion products build up in the thin igniter tube. The purge flow significantly increased the total flow rate such that the N_2 mass flow rate was anywhere from 40-70 percent of the total engine flow rate. Figure 4 shows the effect of the added nitrogen flow on the chamber mixture ratio. The O/F is plotted versus the chamber mixture ratio (O/F_C), where the O/F_C is computed assuming that the nitrogen flows are "fuels" and this mass flow is in the denominator or:

$$O/F_C = \frac{\text{Oxidizer flow rate}}{\text{Fuel flow rate} + N_2 \text{ purge flow rate}}$$

In the figure, it is clear that the O/F can be seriously affected by the nitrogen purge flow. All of the cases, regardless of O/F, are strongly influenced. These purge flow rates were included in all of the I_{sp} calculations, and the added nitrogen does significantly reduce the overall engine I_{sp} . Table III shows a typical case for the 55-wt% RP-1/Al. The total N_2 flow in the engine caused the overall O/F to be 0.24, whereas the main combustion flow had an O/F of 2.00. Though the high N_2 flow was not the only contributing factor, the overall result was Cstar efficiency for the engine of only 47%.

Also during the testing, there tended to be a small buildup of gelled fuel in the converging region and this buildup was, in part, from the small amount of fuel that flowed from the injector after engine had shut down. The residual pressure in the fuel manifold forces this small amount into the chamber. With the engine mounted horizontally, this buildup of propellant was located primarily on the lower portion of the nozzle's converging section and the buildup reached a maximum amount in the nozzle. This buildup had several noticeable effects on the combustion. When firing the gelled fuel with 0- and 5-wt% RP-1/Al, the bottom of the exhaust plume tended to appear clear, while the upper portion was much more optically thick or white. This propellant buildup seemed to sweep particles out of the lower part of the plume. The effects of this sweeping may be the cause of the somewhat larger dispersions in the I_{sp} efficiencies of the 0- and 5-wt% RP-1/Al tests when compared with the ungelled RP-1 and 55-wt% RP-1/Al.

Heat Transfer and Combustion Experiments: Results, Discussion, and Observations

Engine Performance and Efficiency

The results presented here are based on initial analyses of the test data. All of the results presented here are for the heat sink engine. The overall I_{sp} , Cstar efficiency, I_{sp} efficiency, and other important data are presented to show some of the important features and potential difficulties with metallized gelled fuels. The theoretical engine performance¹⁵ was calculated using a standard rocket performance computer code for each fuel type and it is used to estimate the I_{sp} and Cstar efficiencies.

The simplified computations for I_{sp} , Cstar efficiency and I_{sp} efficiency are shown below:

Experimental Vacuum Specific Impulse.

$$IVT = \frac{F}{WTOT} \quad (lb_f \cdot s / lb_m)$$

where:

IVT = Experimental Vacuum Specific Impulse

F = Thrust level

WTOT = Total Mass Flow Rate in the Engine
(including N₂ purges)

$$F = CF * P_c * MPL * AT$$

where:

CF = Thrust coefficient at nozzle exit (using
Ref. 22)

P_c = Chamber Pressure

MPL = Momentum Pressure Loss

AT = Throat area

Cstar efficiency.

$$CSXP = \frac{P_c * MPL * AT * G}{WTOT} \quad (\text{ft/s})$$

where:

CSXP = Experimental Cstar

G = Gravitational Constant

NCSP. C-star efficiency (based on
chamber pressure)

$$NCSP = \frac{CSXP * 100}{CST} \quad (\%)$$

where:

CST = Cstar predicted using Ref. 15

I_{sp} efficiency.

$$NISPP = \frac{IVT * 100}{IVAC} \quad (\%)$$

where:

NISPP = I_{sp} efficiency

IVAC = theoretical vacuum specific impulse
predicted using Ref. 22.

Heat Transfer Calculations

The simplified heat transfer
computations are described below (Ref. 17-
20). The average heat flux per segment is:

$$Q_n = \frac{WCOOL * C_p * DT_n}{ARCOOL}$$

where:

Q = heat flux for segment n
(MW/m²)

WCOOL = coolant flow rate per segment
(kg/s)

C_p = Specific heat of water
DT = temperature rise for
segment n (temperature in K)

ARCOOL = surface area cooled by
segment n (m²)

Engine I_{sp} and Efficiency

The preliminary test results of I_{sp}, Cstar
efficiency and I_{sp} efficiency are plotted versus
the main combustor O/F range tested for each
fuel and these figures are described in the
succeeding sections. The O/F provided in the
figures is the main combustor O/F, and not
the chamber O/F (O/F_C) described in a
preceding section. In each set of data for the
gelled fuels, there is a wider range of variability
than that seen with the ungelled RP-1. This
variability is caused by the deposits of metal in
the chamber and the nozzle, the erosion of the
injector, and the potential of gelled propellant
density variations as the propellant flowed
through the feed system to the injector. This
introduced some uncertainty in the mass flow
rate, but these were small after gaining
experience with the feed system. These effects
are described in the section on observations.

Figures 5, 6, and 7 summarize the
results. In Figure 5, the maximum I_{sp}
produced by each fuel and the range of I_{sp}
variation near the maximum value are shown.
The theoretical predictions, which included the
nitrogen purge flow, do not precisely match
the experimental trends for the 0- and 5-wt%
RP-1/Al. The trend is not concerning the
values of the I_{sp}, but the relation between the
different values. With the 0- and 5-wt% RP-
1/Al, the theoretical trend is a small increase in
I_{sp} for both of these fuels over RP-1 and a
reduction in I_{sp} for the 55-wt% RP-1/Al.
While a small increase in I_{sp} was predicted for
the 0- and the 5-wt% RP-1/Al, there was no
increase in I_{sp} for the 0-wt% RP-1/Al over RP-

1 that is demonstrated in the experimental data. There is, however, a very small increase in the experimental I_{sp} going from the 0-wt% RP-1/Al to the 5-wt% loading, consistent with the predicted theoretical trend. The 55-wt% RP-1/Al follows the reduced I_{sp} trend noted in the theoretical predictions.

Figure 6 shows the Cstar efficiency ranges (near the maximum I_{sp} values) from the experiments. All of the fuels showed a low upper bound on the Cstar efficiency: from 47 percent (55-wt%) to 69 percent (RP-1). The RP-1 varied from 65 to 69 percent and the gelled RP-1 (0 wt%) had a range of 60 to 62 percent. The 0-wt% RP-1/Al showed the smallest variation in the efficiency. With the 5-wt% fuel, the dispersion in efficiency was from 65 to 67 percent, while the 55 wt% variability was 42 to 47 percent. A summary of the I_{sp} efficiency is presented in Figure 7 and all of the gelled fuels had similar variations in the efficiency data. The RP-1 efficiency only varied from 55-61 percent, while the gelled RP-1 (0 wt%) efficiency ranged from 52-53 percent. The other fuels had a slightly broader range of variation, with 52 to 58 percent with the 5-wt% RP-1/Al and 36 to 40 percent with the 55-wt% fuel.

O₂/RP-1.

Figure 8 presents the I_{sp} versus O/F for the O₂/RP-1 engine. The maximum I_{sp} for the RP-1 was 125.6 lb_f-s/lb_m and was located near an O/F of 4.2. This maximum value is different from the typically computed maximum near 2.7 for O₂/RP-1¹¹. The difference is due to the added nitrogen purge gas in the flow. The Cstar efficiency is plotted versus O/F in Figure 9. With the O₂/RP-1, the maximum Cstar efficiency was 69%. The I_{sp} efficiency is shown in Figure 10 and, for the RP-1 (ungelled), the maximum efficiency was 61%.

RP-1/Al: 0-wt% Al.

In Figure 11, the I_{sp} of the 0-wt% RP-1/Al engine is provided. The maximum I_{sp} for the 0 wt% RP-1/Al was 114.5 lb_f-s/lb_m and was at an O/F of 2.6. Figure 12 illustrates the

engine's Cstar efficiency which was a maximum of 62% at an O/F of 2.6. The maximum I_{sp} efficiency for the 0-wt% RP-1 was 53% and the data for the range of O/F ratios are shown in Figure 13.

RP-1/Al: 5-wt% Al.

As shown in Figure 14, at a 5 wt% RP-1/Al loading, the maximum I_{sp} occurred at an O/F of 2.0 and was 127.1 lb_f-s/lb_m and the lowest I_{sp} at this O/F was 97.3 lb_f-s/lb_m. Also, the performance has a band of variability at the maximum of the O/F range, but the variation is narrow and the performance was more repeatable compared to the 0-wt% and 55-wt% RP-1/Al. Using 5-wt% O₂/RP-1/Al, a range of 65 to 67% Cstar efficiency was delivered. The efficiency data, provided in Figure 15, was relatively constant over the range. The I_{sp} efficiency, depicted in Figure 16, had a maximum of 58% at an O/F of 1.3.

RP-1/Al: 55-wt% Al.

As shown in Figure 17, at a 55 wt% RP-1/Al loading, the I_{sp} peak occurred in the range of an O/F of 2.0. The peak I_{sp} was 79.7 lb_f-s/lb_m at an O/F of 2.0. Also, the performance varied over a relatively narrow range over the entire range of O/F. Figures 18 and 19 show the Cstar efficiency and I_{sp} efficiency versus O/F for 55-wt% gelled RP-1/Al, respectively. The Cstar efficiency for this propellant was 47% (at an O/F of 2.0) and low as 42% at a similar O/F. With I_{sp} efficiency, the values ranged from 40% at an O/F of 2.0 and the lowest value at that O/F is 36%.

Heat Transfer Results

The heat transfer results are presented in the Figures 20-22 in which the results for RP-1 are compared with each gelled fuel type. These figures include the heat flux values versus distance from the injector face for the four fuels. The highest heat flux occurs at cooling channel station 28, which was just upstream the nozzle throat, 20.6 cm from the injector face. In each of the cases presented in the heat flux analyses, the values were the

representative cases for each fuel type, and not necessarily the highest heat flux or the highest I_{sp} . For the 55-wt% RP-1/Al, the highest I_{sp} case for this fuel was one of the lowest peak heat fluxes for the 55-wt% fuel. The formation of a metal oxide coating in the nozzle in the 55-wt% cases led to a reduction in the flux and this reduction will be discussed in the succeeding sections.

During the calorimeter firings, the temperature of the cooling water did not always increase as expected. It was found later through inspection of the test photos taken during some the firings with lower chamber pressures that the rocket exhaust flow was separating from the nozzle. The heat transfer beyond that separation point was minimal and explains, in part, the fast drop in heat flux for the last two cooling channels in the heat transfer analyses. Past testing also shows that the nozzle heat flux will drop quickly after the peak nozzle heat flux.¹⁸ Flow separation did not occur in all of the test runs, but it is noted as part of the explanation of the low nozzle heat fluxes.

RP-1

Figure 20 provides an RP-1 heat flux profile (Run 873). The nozzle section near the throat had the highest heat flux. This result is typical of past testing.¹⁷⁻²⁰ A stable combustion zone established itself between the 3 and 7 cm region. After the heat flux reaches 1.7 MW/m^2 , the flux is nearly constant until the flow enters the nozzle. The peak heat flux was 3.6 MW/m^2 and occurred at cooling channel station 28, 20.6 cm from the injector face and just upstream of the nozzle throat. The last two stations (see Table II) show a very low flux because the flow became separated from the nozzle and therefore the flux drops off very quickly.

0 wt% RP-1/Al

Figure 20 compares the RP-1 (Run 873) and 0-wt% RP-1/Al heat flux profiles (Run 908). The 0-wt% RP-1/Al heat flux near the injector face is low, due to the time and

distance required to establish the combustion zone, and also due in part to the deposition of partially combusted gelled fuel at the injector chamber interface. A combustion delay is implied in the figure, with the heat flux near the injector being lower than the RP-1. Figure 21 shows the reduction in heat flux for a set of runs for RP-1 and 0-wt% RP-1/Al. Q/A(1) and Q/A(2) in the figure are the first two cooling circuits nearest the injectors face. It is apparent that the overall flux for these two circuits in the 0-wt% RP-1/Al cases (Runs 901-958) are substantially lower than the corresponding values for RP-1 (Runs 747-900).

After the initial low Q/A values, the flux increased to 2.3 MW/m^2 , an increase due to the combusting SiO_2 gellant, and then the flux dropped below the RP-1 heat flux value to a low point of 1.0 MW/m^2 . This drop in heat flux implies that the chamber coating of partially combusted fuel had formed and is cooling the latter part of the chamber. The peak nozzle heat flux was 3.9 MW/m^2 .

5 wt% RP-1/Al

Figure 22 depicts the RP-1 (Run 873) and 5-wt% RP-1/Al (Run 986) heat flux profiles. As with the 0-wt% case, the heat flux has a profile where the flux is slightly lower than the baseline RP-1 value near the injector face, reached a peak in the chamber at 5 cm from the face, dropped below the RP-1 flux in the last part of the chamber, and reached a final highest peak just before the nozzle throat. The peak flux in the nozzle was 6.5 MW/m^2 . We can infer that the coating of partially consumed gel in the chamber reduced the heat flux in the second half of the chamber.

55 wt% RP-1/Al

Figure 23 shows the heat transfer profiles for RP-1 (Run 873) and the 55 wt% RP-1/Al (Run 1019). The nozzle station 28 near the throat had the highest heat flux (6.7 MW/m^2), and this flux is the highest of all the cases. Higher heat fluxes were also observed in other 55-wt% cases. Figure 24 compares

the peak nozzle heat flux for 12 different runs. The Q/A variation is due to the thin metal oxide coating that formed on the nozzle surface, insulating the nozzle wall from the combustion gases. The values where the flux dropped and then returned to a high peak are cases where the oxide coating was removed after it had built up on the nozzle surface. After runs 1013 and 1017, the build-up of the oxide was removed with a small chisel. After run 1013, a large fraction of the coating could be removed and the heat flux returned to a high value on the next run. It was clear that after run 1017, though the coating was removed from the throat and diverging section of the nozzle, much of the coating remained on the converging section of the nozzle. This remaining coating caused the reduction in the heat flux noted in Figure 24.

Metal agglomerations in the nozzle.

When testing the 55-wt% RP-1/Al, metal agglomerations occurred in the nozzle. This same effect occurred with the heat-sink engine. We wished to avoid this buildup with the calorimeter testing and therefore cleaned the nozzle surface and removed the Al₂O₃ as quickly as possible after each run. An attempt was made to combat the agglomerations by firing the engine igniter to eradicate the small nozzle agglomerations as they formed. The agglomerations were reduced in magnitude over those formed with the heat sink nozzle. Instead of a thick coating that narrowed the nozzle throat, only a very thin coating of a few millimeters in thickness formed. This agglomeration was a hardened metal buildup that could not be easily removed. After taking the nozzle off the test rig, the agglomeration could be chipped off with a chisel and once loosened, came off in large segments. During the previous heat sink engine testing, (after 15, 2-second firings), the agglomeration had reduced the throat diameter from 0.6 inches to 0.45 inches.

Discussion

Some of the engine performance numbers appear to be very low. These low values are the result of the extremely high

fraction of nitrogen in the engine flow. The high nitrogen flow rate was used to protect the O₂/H₂ igniter in the center of the injector. Due to several difficulties with flow rate computations and measurements, these very high nitrogen flows were used in the engine. The nitrogen has two effects: reducing inter-element mixing and lowering the combustion temperature, which may slow the vaporization of the RP-1. The predicted chamber gas temperature for the O₂/RP-1 case using the high nitrogen mass flow was 2651 K (O/F = 0.44). Using O₂/RP-1 with no nitrogen purge, the chamber gas temperature was 3308 K (O/F = 2.6). This temperature drop may have a significant effect upon the vaporization and combustion efficiency of the RP-1. The nitrogen purge flow for the engine's igniter was down the center of the chamber, with the 4 or 8 O-F-O elements surrounding the igniter. The nitrogen could then tend to isolate some of the elements from one another. The RP-1 vaporization length was assessed using a code named ROCCID.²³ This code predicted a 72% combustion efficiency for this 5.875-inch chamber with O₂/RP-1. The short chamber implies a lower vaporization level for the RP-1, and hence a reduced Cstar efficiency and performance. The short chamber was used because of the availability of the calorimeter chamber. Based on this analysis, the low performance could be increased by increasing the chamber length.

Another effect that may have lowered the engine performance is injector design. A typical O₂/RP-1 injector operates at an O/F of 2.6 to 2.7. The O₂/RP-1 injector was designed to operate over a range of 3.4 to 4.2 O/F, so that a wide range of testing could be conducted with a single injector. This design produced an injector with an oxidizer post diameter of 0.144 inches and a fuel post diameter of 0.0225 inches. These larger O₂ posts may have led to inefficient mixing of the RP-1.

Analyses show that the heat transfer to the wall was significantly different for the RP-1/Al at 55-wt% versus the RP-1 fuel. Also, a gellant and an aluminum combustion delay was inferred in the 0% and 5-wt% RP-1/Al cases

from the decrease in heat flux in the first part of the chamber. A large decrease in heat flux in the last half of the chamber was caused by fuel deposition in the chamber and nozzle. The engine combustion occurred well downstream of the injector face based on the heat flux estimates from the temperature measurements. This location of the combustion zone and the deposition of partially combusted fuel on the walls may have led to some of the reduction in the expected performance.

Observations

Heat Transfer and Potential Chamber Cooling Effect

The 0-wt% RP-1/Al case showed the potential insulation and cooling effect of the deposition of partially combusted fuel on the chamber walls. In Figure 25, the wall temperatures for the RP-1 and 0-wt% cases are shown. In three of the last five temperature stations, the 0-wt% case has a lower wall temperature than the RP-1 case. During inspection of the chamber during firings and after disassembly, a thin layer of partially combusted propellant coats the chamber and nozzle, which is discussed in the next section. A similar coating of the engine had occurred with the previous heat sink engine testing.¹⁵⁻¹⁶ An improved cooling technique might be derived from this effect, but additional analyses of the data are required.

Self-protection of injectors

During the testing with gelled RP-1 and the 5-wt% RP-1/Al, some residual propellant was found in the rocket chamber, coating the entire injector face and all of the chamber walls. This residual propellant was actually a mix of unburned fuel (with a gray or clear pink color) and some black or combustion products. Figure 26 shows the typical shape of the fuel deposits. This effect was perhaps due to the fuel lead of 0.2 to 0.3 seconds used in the ignition sequence of the engine. After many firings, this added propellant did not completely undergo combustion, and formed this smooth layer on all the internal surfaces.

Once this thin layer was removed with a soft cloth, the metal surfaces exhibited minimal erosion. An improved cooling technique might be derived from this effect. After further analysis of the heat transfer data, a strategy might be formed to use this effect to improve engine lifetime.

With the ungelled RP-1 and 55-wt% RP-1/Al, there was no protective effect layer formed. There was discoloration and blackening of the O₂/RP-1 injector faces and injector-face erosion, pitting, and metal deposition that occurred with the 55-wt% RP-1/Al. The greatest damage was done to the 55-wt% RP-1/Al injectors after they had been used, removed, cleaned, and replaced in the engine. Residual metal particles that had been retained in the O₂ manifold and the other injector flow passages were areas where O₂ attacked the metal and, in some cases, caused severe injector damage.

Other Gel Effects in the Chamber

Slumping of the gel in the chamber after a firing did cause some unusual plume shapes during the rocket experimental runs. Buildup of a layer in the chamber occurred in the converging section of the previous heat sink firings and also in the current calorimeter tests. There were longer times between firings with the calorimeter due to the need to recharge the water cooling system and the time to estimate the uniformity of the temperature profile in the chamber. These longer down times where the gel is allowed to flow down the chamber walls may have caused this slumping and buildup.

Propellant Drying in the Injector

Using the igniter to clear the nozzle agglomerations also tended to evaporate the liquid component of the gelled fuel during testing of the 55% RP-1/Al with the calorimeter. A relatively dry RP-1/Al residue would form in the fuel ports and the fuel dome. This result is however confounded with the fact that the injector had not been changed for three successive propellant types being tested: 0%, 5%, and 55% RP-1/Al. The injector was left in

place over multiple propellant changes because of the complexity of removing it. Although the engine and injector were thoroughly flushed with Solvent 140 and nitrogen purges, some buildup of gelled 0-wt% RP-1 dry residue (pink gel only) was evident in the fuel dome once it was disassembled (5 to 10% by volume). This residue is partially attributed to the drying effect of the igniter on the fuel in the injector.

Firings with the 55% RP-1/Al resulted in repeatable performance, but the injector erosion was the greatest of any of the tested fuels. Improving the cleaning process of the O₂ manifolds, or preventing the flow of particles into the manifolds would allow more cost effective and longer-lived testing of the 55-wt% RP-1/Al. More easily disassembled manifolds and injectors would allow better access to flow passages that would trap metal particles. Prevention of the deposition of dried metal particles onto all engine surfaces will be very important for future high metal loading metallized propellant testing programs, not to mention any operational propulsion systems.

Conclusions

Rocket engine performance and heat transfer were determined with a calorimeter combustion chamber and nozzle using RP-1 and metallized gelled RP-1/Al fuels. Rocket combustion performance was not as expected, due to gelled fuel deposition in the combustion chamber, a shorter than desired chamber length, and a high nitrogen purge flow for the engine's igniter. The combustion of metallized gelled propellants was realized with even simple 4- and 8-element triplet injectors. Rocket Cstar efficiency for the RP-1 fuel was in the 65-69% range, while the gelled 0-wt% RP-1 delivered 60 to 62% Cstar efficiency. The 5-wt% RP-1 exhibited a Cstar efficiency range of 65 to 67% and the 55-wt% RP-1 fuel delivered a 42 to 47% Cstar efficiency.

The deposition of uncombusted fuel in the chamber had a very strong influence on the heat flux profiles in the 0-, 5- and 55-wt% RP-1/Al cases. The highest heat flux in the chamber was 1.7 MW/m² for the RP-1, 2.3

MW/m² for 0-wt% RP-1/Al, 2.8 MW/m² for the 5-wt% case, and 3.6 MW/m² for the 55-wt% fuel. After the initial high heat flux in the first half of the chamber, the heat flux would drop rapidly in the second half of the chamber, dropping from their high values to about 1.0 MW/m² for the 0- and 5-wt% cases, and 2.5 MW/m² for the 55-wt% RP-1/Al. Inspection of the chamber after each firing showed that fuel had deposited along the walls, causing the flux to drop. After leaving the chamber, heat transfer measurements with RP-1, 0-, 5-, and 55-wt% RP-1/Al gelled fuels showed that the peak nozzle heat flux for some cases were double that of the RP-1 fuel combustion, especially with the 55-wt% RP-1/Al.

Concluding Remarks

Though the high metal loading, 55-wt% RP-1/Al, engine runs experienced some agglomeration and erosion difficulties, the 0- and 5-wt% tests ran well, with a Cstar efficiency similar to the RP-1, and demonstrated a self-protective layer of gelled propellants and combustion products. The most interesting results occurred with the 0% and 5% RP-1/Al formulations. A thin layer of gelled fuel and combustion products formed throughout the chamber and protected the face of the injector from virtually all burning, scoring, or other damage.

Many additional analyses can be conducted on the heat transfer characteristics of these engines. The time dependence of the combustion and heat transfer has not been fully investigated, the potential metal combustion lag due to gelled and metallized gelled fuels has only been analyzed in a preliminary manner, and much additional analysis of the data can provide many more insights. This work would help improve the engine designs and eliminate the losses due to fuel deposition.

Though the performance obtained with the metallized gelled fuels is lower than that required for beneficial applications to NASA missions, these results show the ways of improving future engine designs. Historical data with metallized gelled fuels has implied

that engines at higher thrust levels are able to deliver the required high efficiency and I_{sp} . Larger scale experiments will likely allow more realistic flow conditions, reduced influence of igniter purges, and allow researchers to gather more engine data in a more-representative high-thrust rocket environment.

These first rocket heat transfer experiments with RP-1/Al were a focus for learning about and documenting the actual rocket performance and any potential operational pitfalls. This work is an ongoing set of analyses to determine the viability of gelled propellants and their possible applications to NASA missions. Continuing system studies will use the data from these and other experiments to find the appropriate uses of metallized gelled propellants.

Acknowledgements

We'd like to thank NASA Headquarters, Office of Space Access and Technology for their support of this work. Also, many thanks to Paul Molnar for his mechanical skills and the team of Bill Furfaro, Ed Pluta, Pablo Gutierrez, and Steve Culler for their electronics experience and assistance. Also, thanks to John Blankenship for his injector design work. Also, particular kudos to Diane Linne, Jack Reed, Gayle Roth, Jack Swoboda, and Joe Zoeckler.

References

- 1) Sanger, E., Raketenflugtechnik, Berlin: R. Oldenberg, 1933, pp. 53.
- 2) Wells, W., "Metallized Liquid Propellants," Space/Aeronautics, Volume 45, June 1966, pp. 76-82.
- 3) Olson, T. and Setze, P., "Some Combustion Problems of High Energy Fuels for Aircraft," NACA Preprint, 1958, International Symposium on Combustion, pp. 883-893 and 7th International Symposium on Combustion, London and Oxford, Aug 28-Sept. 3, 1958.
- 4) Allan, B. and Chew, W., "A Review of Thixotropic Gels for Advanced Propulsion Systems," JANNAP Propulsion Meeting, CPIA Publication 602. Volume III, November 1993.
- 5) Arszman, J. and Chew, W., "TACAWS Propulsion Development Program," JANNAP Propulsion Meeting, CPIA Publication 602. Volume III, November 1993.
- 6) Trikha, A., Warren, S., and Peters, J., "Advanced Crew Escape Capsule Technologies Program," SAFE Association, Newhall, CA Proceedings, 1987, pp. 196-202.
- 7) Palaszewski, B. and Rapp, D., "Design Issues for Propulsion Systems Using Metallized Propellants," AIAA 91-3484, September 1991.
- 8) Rapp, D. and Zurawski, R., "Characterization of RP-1/Aluminum Gel Propellant Properties," AIAA 88-2821, July 1988.
- 9) Mueller, D. and Turns, S., "Some Aspects of Secondary Atomization of Aluminum/ Hydrocarbon Slurry Propellants," AIAA Journal of Propulsion and Power, Volume 9, Number 3, May-June 1993.
- 10) Wong, W., Starkovich, J., Adams, S., and Palaszewski, B., "Cryogenic Gellant and Fuel Formulation for Metallized Gelled Propellants: Hydrocarbons and Hydrogen with Aluminum," AIAA 94-3175, June 1994.
- 11) Palaszewski, B. and Powell, R., "Launch Vehicle Propulsion Using Metallized Propellants," AIAA 91-2050, June 1991.
- 12) Palaszewski, B., "Advanced Launch Vehicle Upper Stages Using Metallized Propellants," NASA TP-3191,

- presented at the JANNAF Propulsion Meeting, Anaheim, CA, October 3-5, 1990.
- 13) Palaszewski, B., "Lunar Missions Using Advanced Chemical Propulsion: System Design Issues," NASA Technical Publication (TP) -3065, AIAA 90-2341, July, 1990, also in AIAA Journal of Spacecraft and Rockets, May-June 1994.
 - 14) Palaszewski, B., "Metallized Propellants for the Human Exploration of Mars," NASA TP-3062, November 1990. Also, AIAA Journal of Propulsion and Power, Nov.-Dec. 1992.
 - 15) Palaszewski, B. and Zakany, J., "Metallized Gelled Propellants: Oxygen /RP-1 /Aluminum Rocket Combustion Experiments," AIAA 95-2435, presented at the 31st AIAA/ASME/SAE Joint Propulsion Conference, San Diego, CA, July 1995.
 - 16) Palaszewski, B., "Metallized Gelled Propellant Experiences and Lessons Learned: Oxygen /RP-1 /Aluminum Rocket Engine Testing," presented at the JANNAF/CPIA Gel Propulsion Technology Symposium, Huntsville, AL, September 1995.
 - 17) Linne, D., "Performance and Heat Transfer Characteristics of a Carbon Monoxide/Oxygen Rocket Engine," NASA Technical Memorandum 105897. February 1993.
 - 18) Quentmeyer, R. and Roncace, E., "Hot Gas Side Heat Transfer Characteristics of a Subscale Plug Nozzle Rocket Calorimeter Chamber," NASA Technical Paper 3380, 1993.
 - 19) Quentmeyer, R., Schacht, R., and Jones, W., "Hot Gas Side Heat Transfer with and without Film Cooling on a Simulated Nuclear Thermal Rocket Thrust Chamber Using H_2-O_2 ," NASA Technical Note, TN D-6638, February 1972.
 - 20) Schacht, R. and Quentmeyer, R., "Coolant Side Heat Transfer Rates for a Hydrogen-Oxygen Rocket and a New Technique for Data Correlation," NASA Technical Note, TN D-7207, March 1973.
 - 21) Starkovich, J., Adams, S., and Palaszewski, B., "Nanoparticulate Gellants for Metallized Gelled Liquid Hydrogen with Aluminum," AIAA 96-3234, July 1996.
 - 22) Gordon, S., and McBride, B., "Computer Program for Calculation of Complex Chemical Equilibrium Compositions, Rocket Performance, Incident and Reflected Shocks, and Chapman-Jouguet Detonations," NASA SP-273, Interim Revision, March 1976.
 - 23) Muss, J., Nguyen, T., and Johnson, C., "User's Manual for Rocket Combustor Interactive Design (ROCCID) and Analysis Computer Program," Volume I - User's Manual, NASA Contractor Report 1087109, NASA Contract NAS3-25556, May 1991.

Table I. Metallized Gelled Fuel Components: Weight Percentages

Metal Loading	Components			
	RP-1	Al	SiO ₂	Surfactant (Tween 85)
0%	93.5	0.0	6.5	0.0
5%	90.0	5.0	5.0	0.0
55%	40.8	55.0	3.5	0.7

Table II
Calorimeter Engine Geometry Data

n	Axial Location from injector face (cm)
Combustion Chamber:	
1	0.546
2	1.458
3	2.093
4	2.728
5	3.363
6	3.998
7	4.633
8	5.268
9	5.903
10	6.538
11	7.173
12	7.808
13	8.443
14	9.078
15	9.713
16	10.348
17	10.983
18	11.618
19	12.253
20	12.888
21	13.523
22	14.158

where: n is the axial station (starting at the injector face)

Table II (continued)
Calorimeter Engine Geometry Data

n	Axial Location from injector face (cm)
Nozzle:	
23	16.027
24	16.939
25	17.851
26	18.763
27	19.675
28	20.587
29	20.978
30	21.951
31	22.939

where: n is the axial station (starting at the injector face)

Table III. Typical Metallized Gelled Propellant Engine Flow Rates and Performance:
55-wt% RP-1/Al, Run 1013

Fluid	Mass Flow Rate (lbm/s, kg/s)	
O ₂	0.0721	(0.0327 kg/s)
RP-1/Al	0.0360	(0.0163 kg/s)
N ₂	<u>0.2603</u>	<u>(0.1181 kg/s)</u>
Total	0.3684	(0.1671 kg/s)
Other parameters for engine run 1013		
Thrust (lb _f , N), vacuum	29.34, (130.5)	
O/F	2.00	
Chamber O/F	0.24	
I _{sp} , (lb _f -s/lb _m , P _c)	79.65	
I _{sp} , vacuum (lb _f -s/lb _m)	201.23	
P _c (psi)	78.91	
Cstar Efficiency	46.57	
I _{sp} Efficiency	39.58	

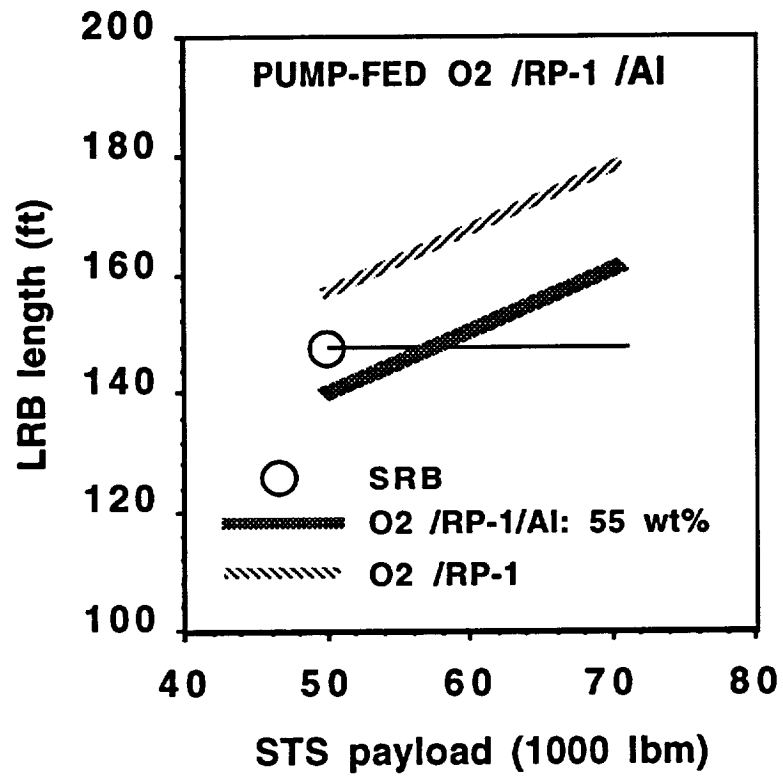


Figure 1. Liquid Rocket Booster Length vs. Payload

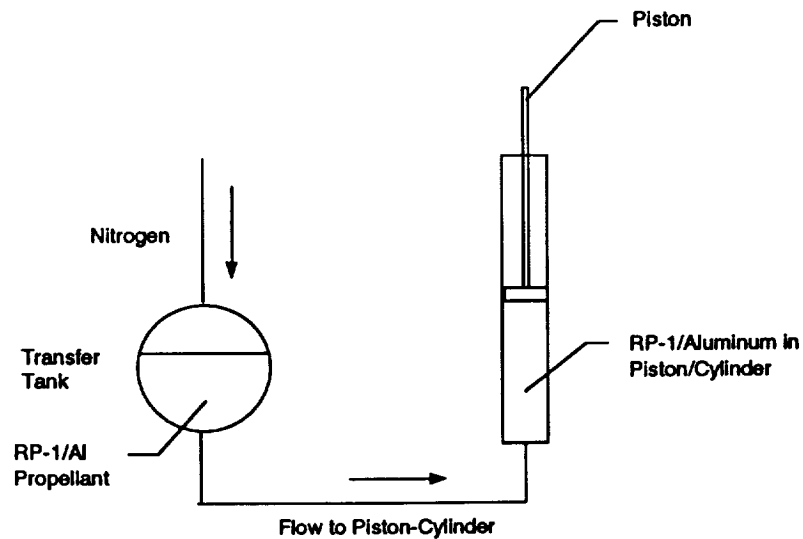


Figure 2. Gelled Propellant Transfer Tank System Schematic

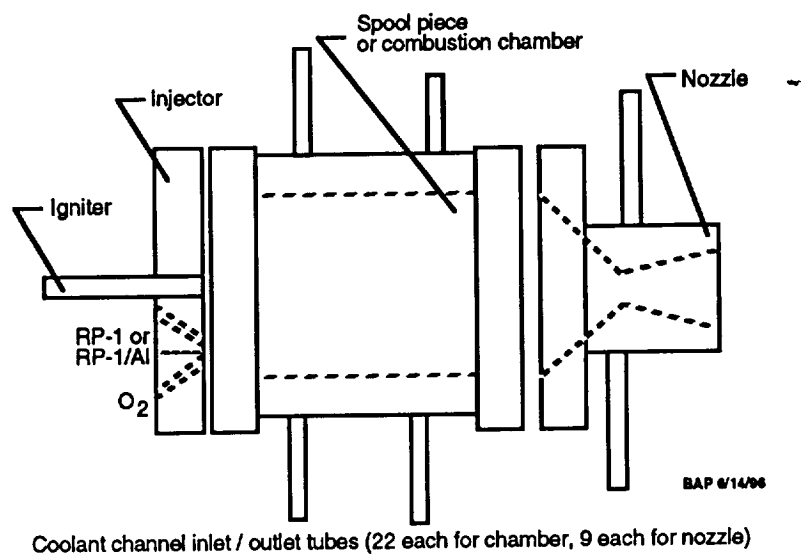


Figure 3. Simplified Diagram of Engine Components and Configuration

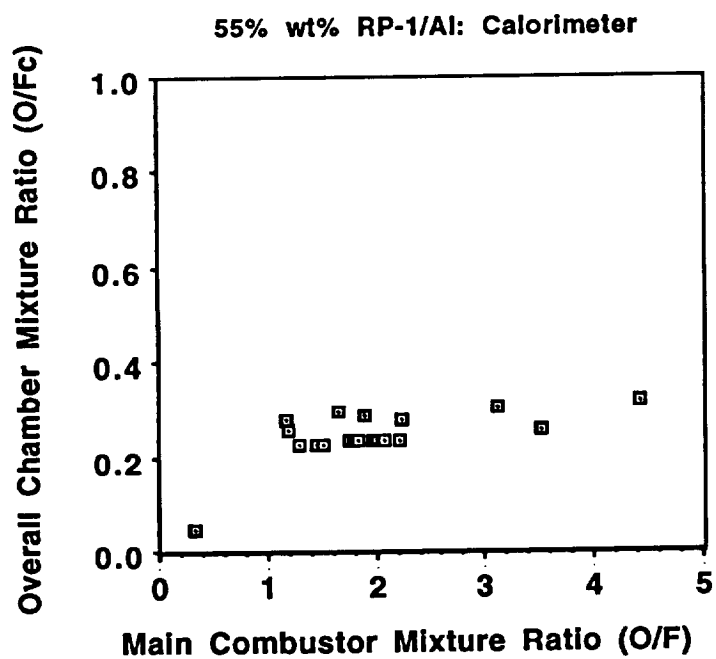


Figure 4. Main Combustor O/F versus Overall Chamber O/F: 55-wt% RP-1/Al with O₂

- Theoretical Vacuum Isp
- △ Test Data: Upper and Lower Bound

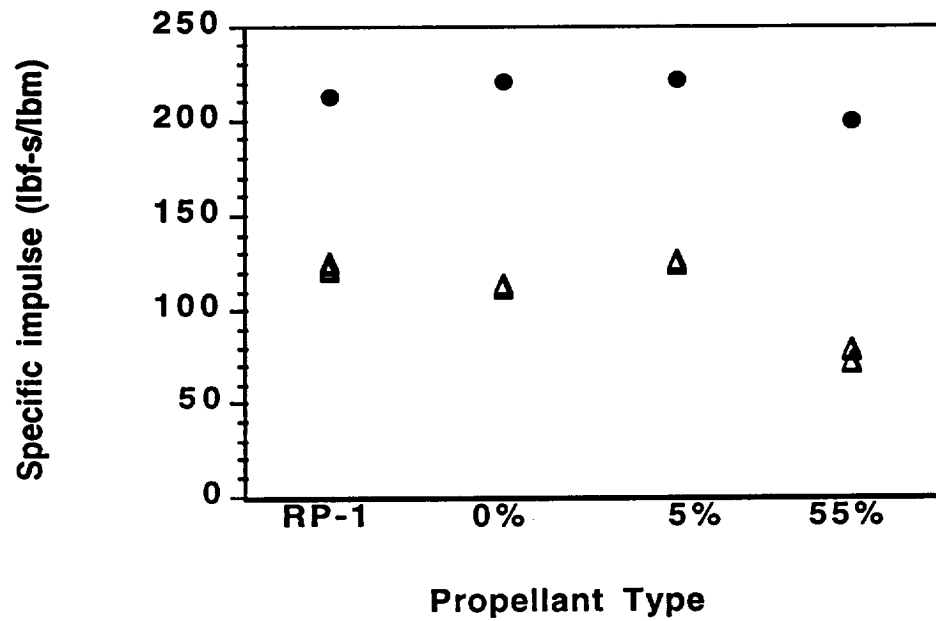


Figure 5. Theoretical and Experimental Peak Isp for all Propellants

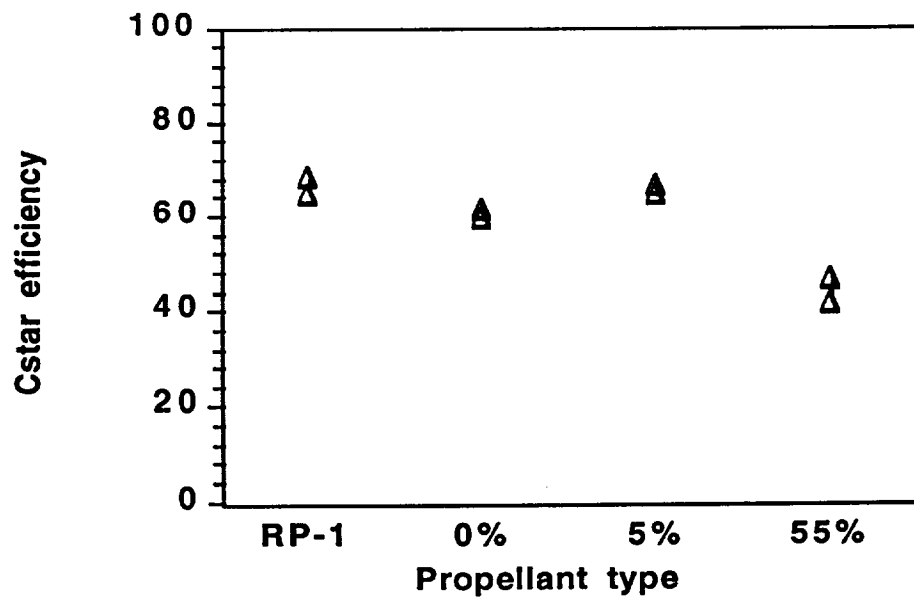


Figure 6. Cstar Efficiency Range Summaries for all Propellants: At Peak Isp

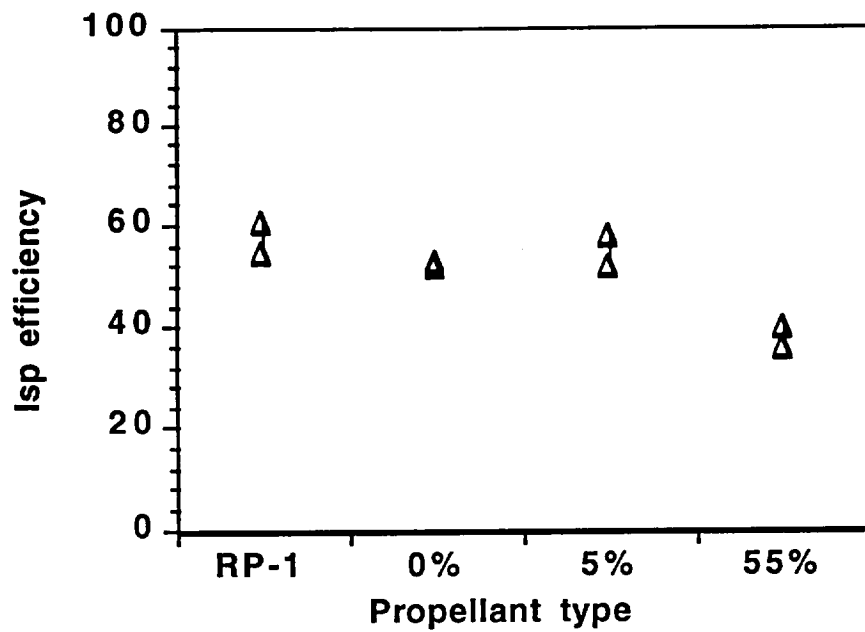


Figure 7. Summary of Isp Efficiency Ranges for all Propellants: At Peak Isp

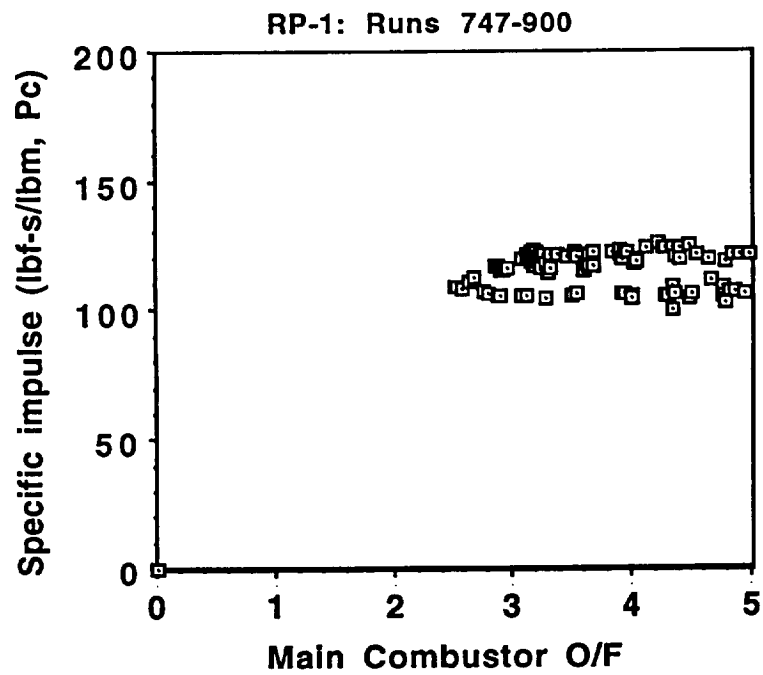


Figure 8. Isp vs. O/F: RP-1 with O₂

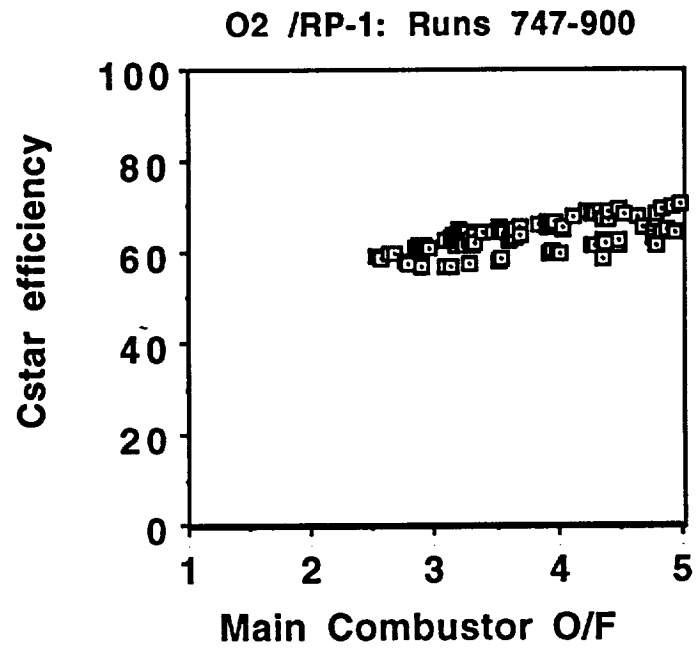


Figure 9. Cstar Efficiency vs. O/F: RP-1 with O₂

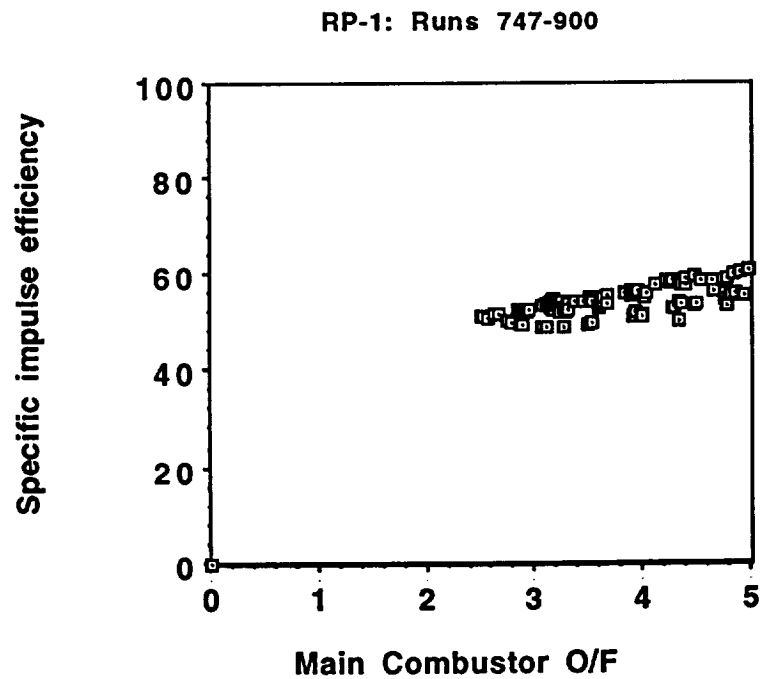


Figure 10. Isp Efficiency vs. O/F: RP-1 with O₂

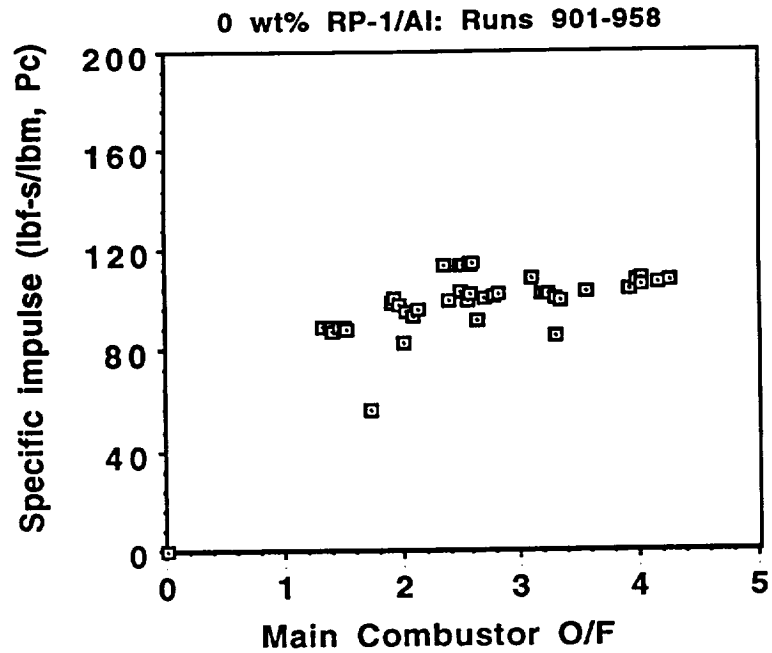


Figure 11. Isp vs. O/F: 0-wt% RP-1/Al with O₂

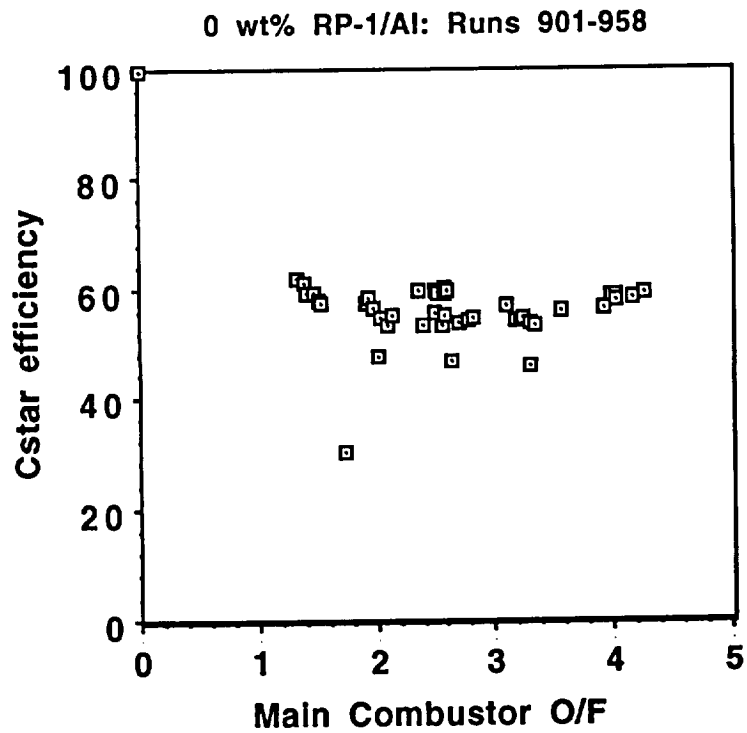


Figure 12. Cstar Efficiency vs. O/F: 0-wt% RP-1/Al with O₂

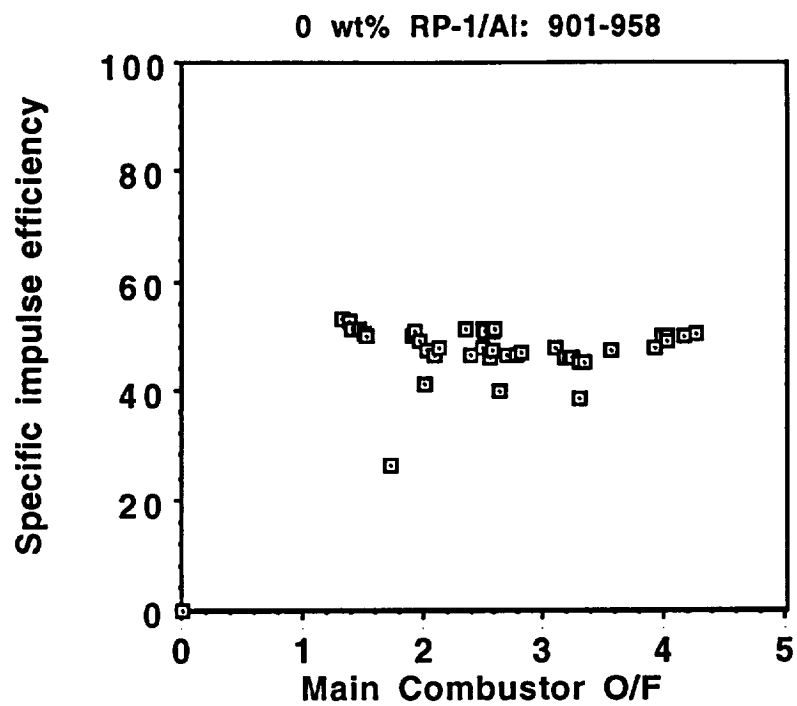


Figure 13. Isp Efficiency vs. O/F: 0-wt% RP-1/Al with O₂

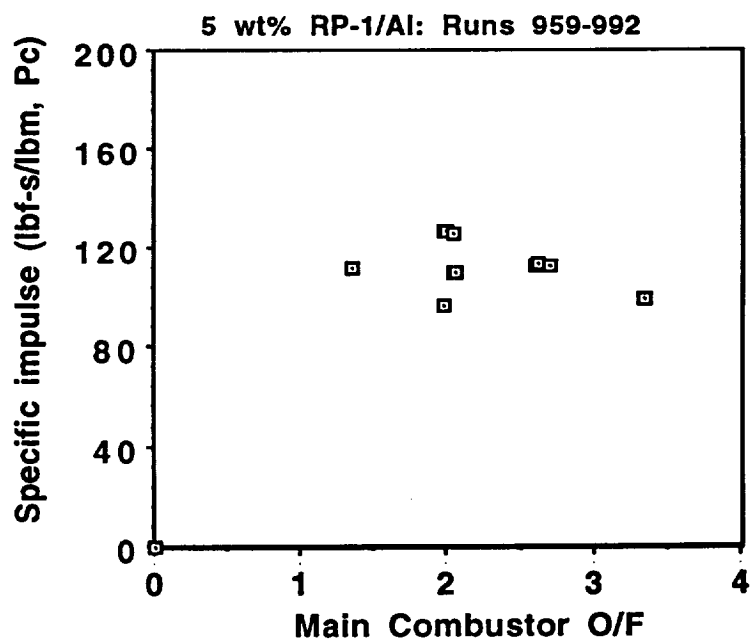


Figure 14. Isp vs. O/F: 5-wt% RP-1/Al with O₂

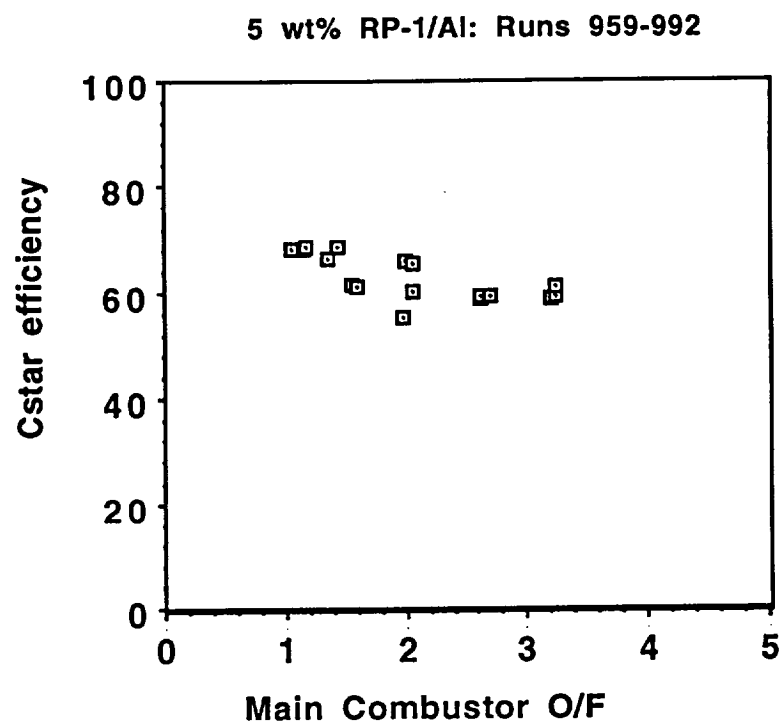


Figure 15. Cstar Efficiency vs. O/F: 5-wt% RP-1/Al with O₂

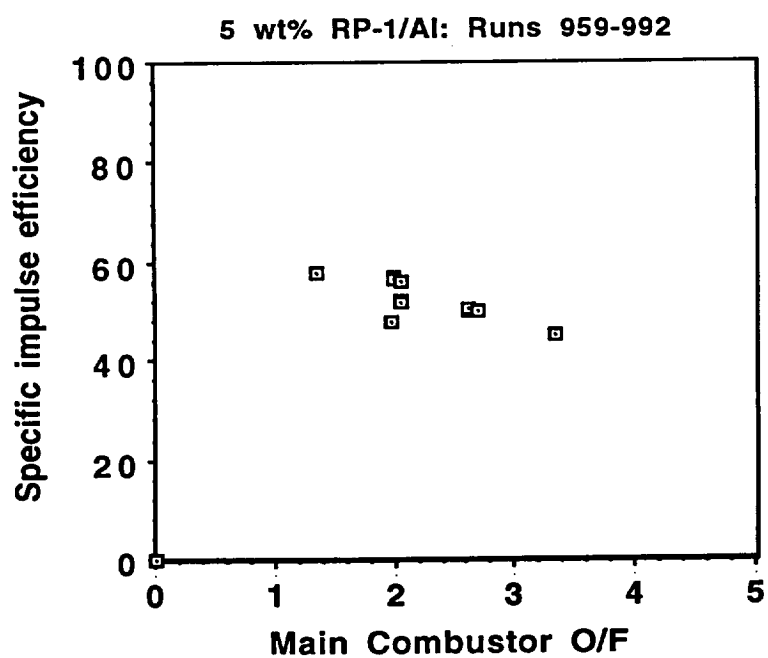


Figure 16. Isp Efficiency vs. O/F: 5-wt% RP-1/Al with O₂

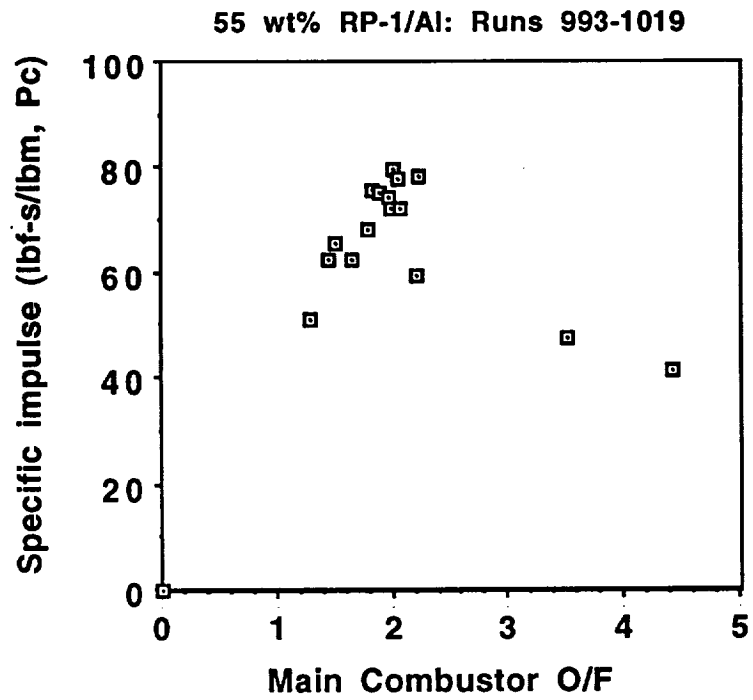


Figure 17. Isp vs. O/F: 55-wt% RP-1/Al with O₂

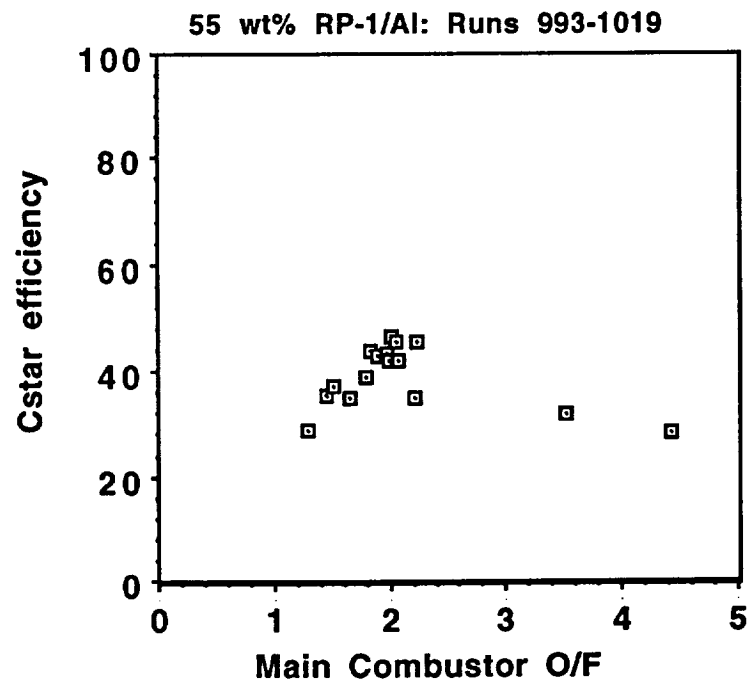


Figure 18. Cstar Efficiency vs. O/F: 55-wt% RP-1/Al with O₂

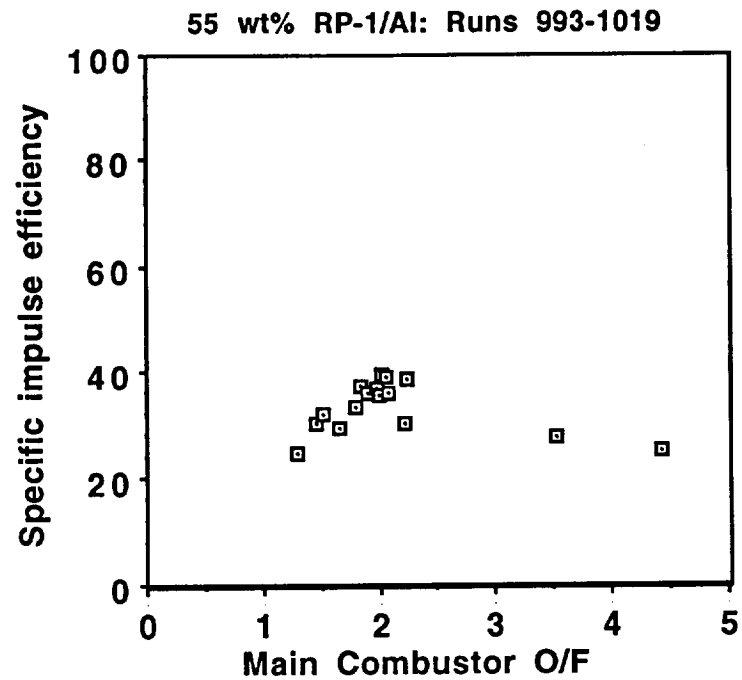


Figure 19. Isp Efficiency vs. O/F: 55-wt% RP-1/Al with O₂

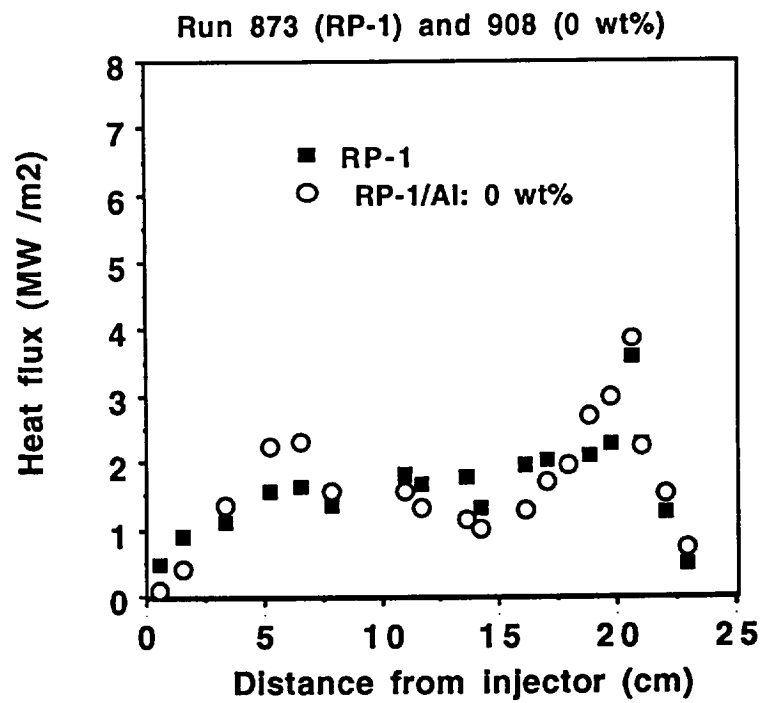


Figure 20. Engine Heat Flux Data: RP-1 and 0-wt% RP-1/Al

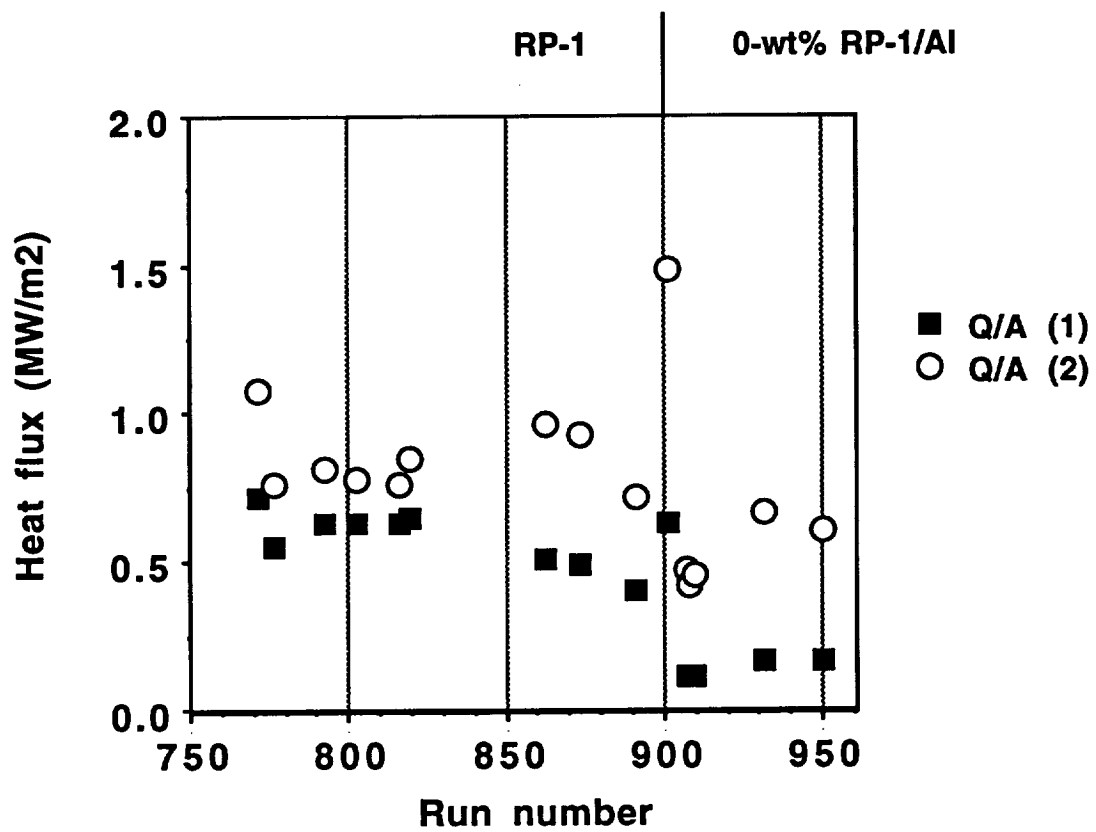


Figure 21. RP-1 and 0-wt% RP-1/Al Heat Flux Comparison: Channels 1 and 2, Nearest Injector

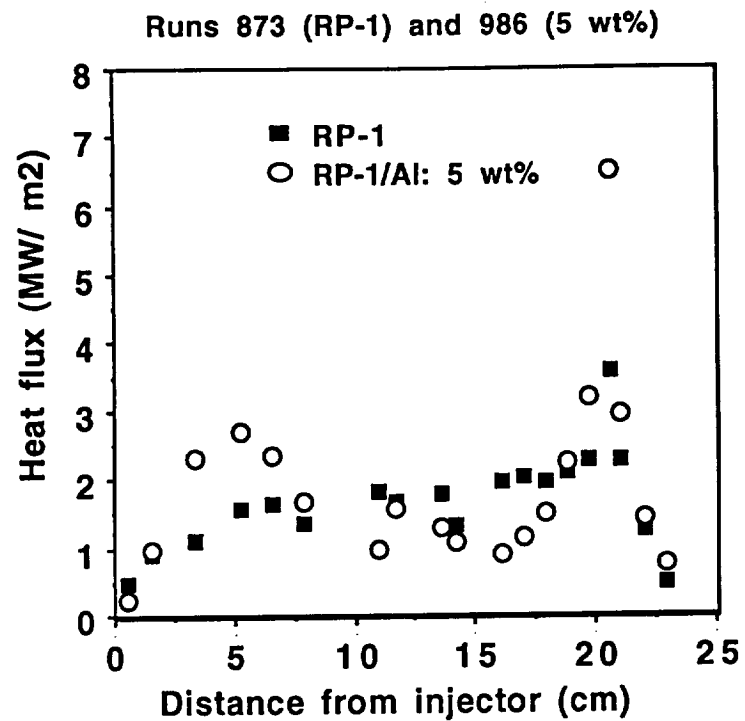


Figure 22. Engine Heat Flux Data: RP-1 and 5-wt% RP-1/Al

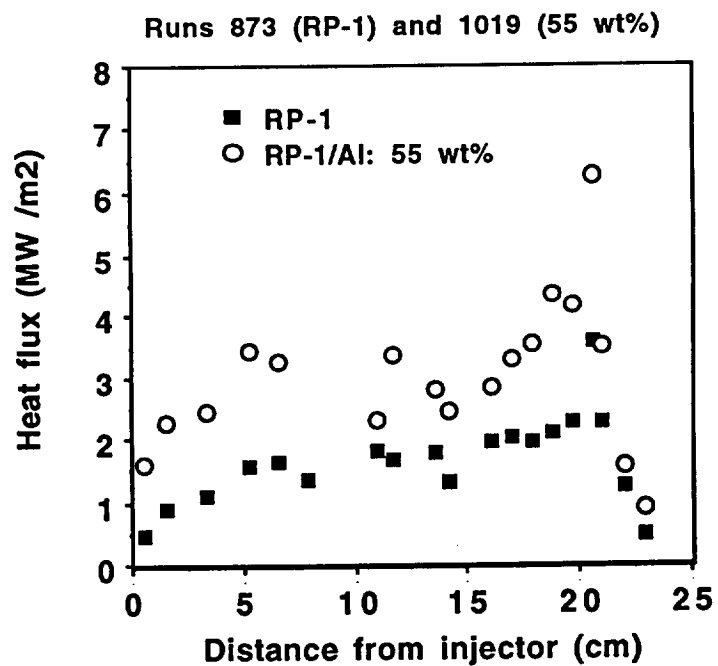


Figure 23. Engine Heat Flux Data: RP-1 and 55-wt% RP-1/Al

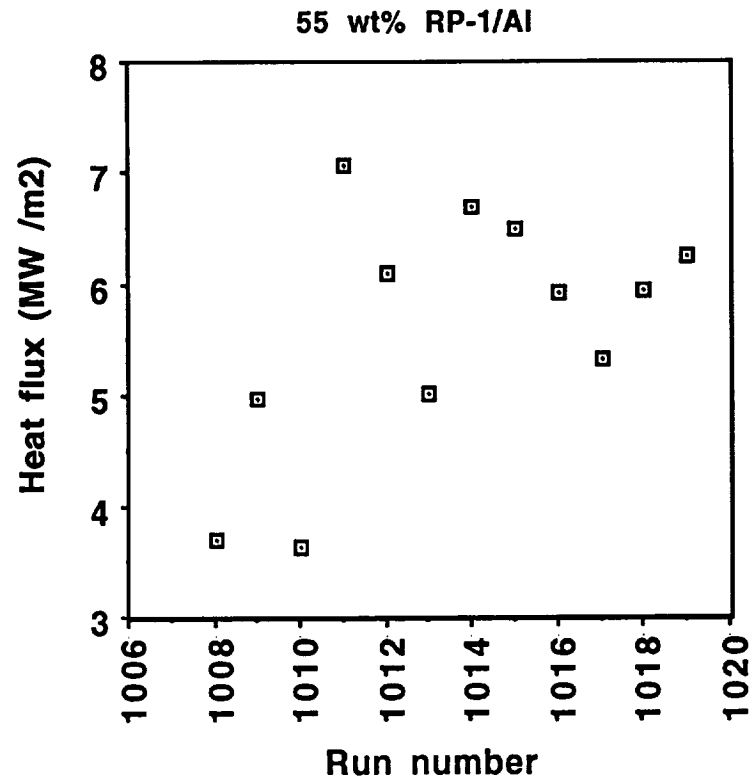


Figure 24. Engine Heat Transfer: Peak Nozzle Heat Flux Data for 55-wt% RP-1/Al

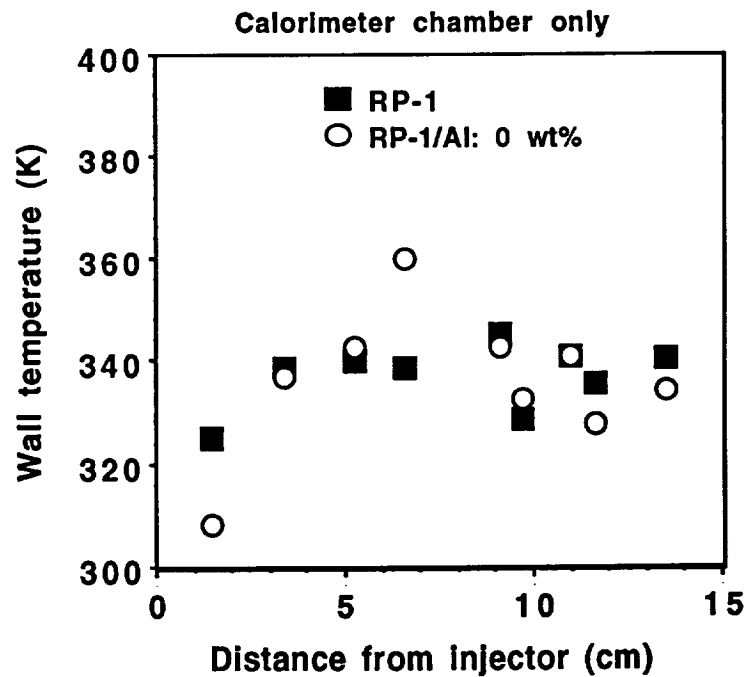


Figure 25. Temperature Profile for RP-1 and 0-wt% RP-1/Al

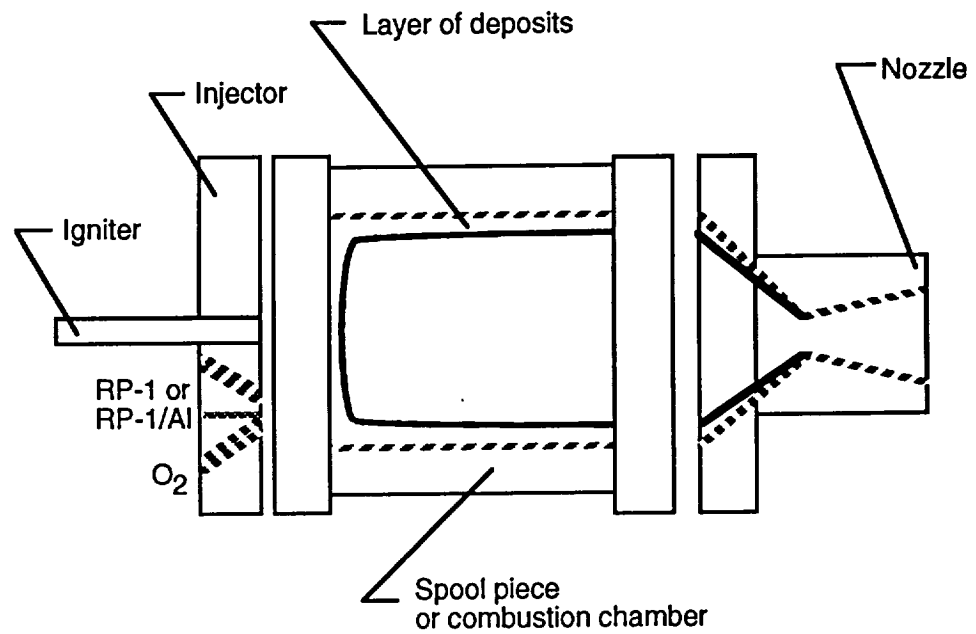


Figure 26. Metallized Gelled Propellant Engine Exaggerated Deposition Illustration

REPORT DOCUMENTATION PAGE			Form Approved OMB No. 0704-0188	
Public reporting burden for this collection of information is estimated to average 1 hour per response, including the time for reviewing instructions, searching existing data sources, gathering and maintaining the data needed, and completing and reviewing the collection of information. Send comments regarding this burden estimate or any other aspect of this collection of information, including suggestions for reducing this burden, to Washington Headquarters Services, Directorate for Information Operations and Reports, 1215 Jefferson Davis Highway, Suite 1204, Arlington, VA 22202-4302, and to the Office of Management and Budget, Paperwork Reduction Project (0704-0188), Washington, DC 20503.				
1. AGENCY USE ONLY (Leave blank)	2. REPORT DATE August 1996	3. REPORT TYPE AND DATES COVERED Technical Memorandum		
4. TITLE AND SUBTITLE Metallized Gelled Propellants: Oxygen/RP-1/Aluminum Rocket Heat Transfer and Combustion Measurements		5. FUNDING NUMBERS WU-252-50-01		
6. AUTHOR(S) Bryan Palaszewski and James S. Zakany				
7. PERFORMING ORGANIZATION NAME(S) AND ADDRESS(ES) National Aeronautics and Space Administration Lewis Research Center Cleveland, Ohio 44135-3191		8. PERFORMING ORGANIZATION REPORT NUMBER E-10400		
9. SPONSORING/MONITORING AGENCY NAME(S) AND ADDRESS(ES) National Aeronautics and Space Administration Washington, D.C. 20546-0001		10. SPONSORING/MONITORING AGENCY REPORT NUMBER NASA TM-107309 AIAA-96-2622		
11. SUPPLEMENTARY NOTES Prepared for the 32nd Joint Propulsion Conference cosponsored by AIAA, ASME, SAE and ASEE, Lake Buena Vista, Florida, July 1-3, 1996. Bryan Palaszewski, NASA Lewis Research Center, and James S. Zakany, NYMA, Inc., 2001 Aerospace Parkway, Brook Park, Ohio 44142 (work funded under NASA Contract NAS3-27186). Responsible person, Bryan Palaszewski, organization code 5310, (216) 977-7493.				
12a. DISTRIBUTION/AVAILABILITY STATEMENT Unclassified - Unlimited Subject Categories 20 and 28 This publication is available from the NASA Center for AeroSpace Information, (301) 621-0390.		12b. DISTRIBUTION CODE		
13. ABSTRACT (Maximum 200 words) A series of rocket engine heat transfer experiments using metallized gelled liquid propellants was conducted. These experiments used a small 20- to 40-lb thrust engine composed of a modular injector, igniter, chamber and nozzle. The fuels used were traditional liquid RP-1 and gelled RP-1 with 0-, 5-, and 55-wt% loadings of aluminum particles. Gaseous oxygen was used as the oxidizer. Three different injectors were used during the testing: one for the baseline O ₂ /RP-1 tests and two for the gelled and metallized gelled fuel firings. Heat transfer measurements were made with a rocket engine calorimeter chamber and nozzle with a total of 31 cooling channels. Each channel used a water flow to carry heat away from the chamber and the attached thermocouples and flow meters allowed heat flux estimates at each of the 31 stations. The rocket engine Cstar efficiency for the RP-1 fuel was in the 65-69% range, while the gelled 0-wt% RP-1 and the 5-wt% RP-1 exhibited a Cstar efficiency range of 60 to 62% and 65 to 67%, respectively. The 55-wt% RP-1 fuel delivered a 42-47% Cstar efficiency. Comparisons of the heat flux and temperature profiles of the RP-1 and the metallized gelled RP-1/A1 fuels show that the peak nozzle heat fluxes with the metallized gelled O ₂ /RP-1/A1 propellants are substantially higher than the baseline O ₂ /RP-1: up to double the flux for the 55-wt% RP-1/A1 over the RP-1 fuel. Analyses showed that the heat transfer to the wall was significantly different for the RP-1/A1 at 55-wt% versus the RP-1 fuel. Also, a gellant and an aluminum combustion delay was inferred in the 0% and 5-wt% RP-1/A1 cases from the decrease in heat flux in the first part of the chamber. A large decrease in heat flux in the last half of the chamber was caused by fuel deposition in the chamber and nozzle. The engine combustion occurred well downstream of the injector face based on the heat flux estimates from the temperature measurements.				
14. SUBJECT TERMS Gelled propellants; Metal propellants; Gellants; Rocket combustion; Metallized gelled propellants; Heat transfer			15. NUMBER OF PAGES 33	
			16. PRICE CODE A03	
17. SECURITY CLASSIFICATION OF REPORT Unclassified	18. SECURITY CLASSIFICATION OF THIS PAGE Unclassified	19. SECURITY CLASSIFICATION OF ABSTRACT Unclassified	20. LIMITATION OF ABSTRACT	

**National Aeronautics and
Space Administration**

Lewis Research Center
21000 Brookpark Rd.
Cleveland, OH 44135-3191

Official Business
Penalty for Private Use \$300

POSTMASTER: If Undeliverable — Do Not Return